Clinical Research Report

Journal of INTERNATIONAL MEDICAL RESEARCH

Journal of International Medical Research
2019, Vol. 47(5) 1975–1986

DOI: 10.1177/0300060519833539
journals.sagepub.com/home/imr
SAGE

Computed tomographic characteristics of gastric schwannoma

Wei Wang[1,2,*], Kaiming Cao[3,*], Yang Han[4], Xiaoli Zhu[2,5], Jianhui Ding[1,2] and Weijun Peng[1,2]

Abstract

Objective: This study aimed to characterize the computed tomographic (CT) features of gastric schwannoma (GS).

Methods: We retrospectively reviewed CT images of 19 cases of histologically proven GS between January 2010 and December 2015. Tumor location, size, contour, margin, growth pattern, and degree and pattern of enhancement, perigastric lymph nodes, ulceration, necrosis, and calcification were evaluated.

Results: GS was located in the gastric body (73.7%), gastric antrum (15.8%), and gastric fundus (10.5%), with a mean maximum diameter of 4.5 ± 1.8 cm. All tumors presented as oval, well-defined solid masses, with exophytic (36.8%), endoluminal (15.8%), or mixed (47.4%) growth patterns. Ulcers (57.9%) and perigastric lymph nodes (47.4%) were observed. Moderate enhancement (87.5%) was observed in the portal phase. Eighteen (94.7%) cases showed homogeneous enhancement.

Conclusions: GS typically presents as a mass in the stomach with an exophytic or mixed growth pattern, moderate homogeneous enhancement, and is prone to be accompanied by perigastric lymph node inflammatory reactive swelling. Larger GSs are more likely to be associated with ulcers.

[1]Department of Radiology, Fudan University Shanghai Cancer Center (FUSCC), Shanghai, PR China
[2]Department of Oncology, Shanghai Medical College, Fudan University, Shanghai, PR China
[3]Department of Radiology, Shanghai East Hospital, Tongji University School of Medicine, Shanghai, PR China
[4]Department of Pathology, Shanghai East Hospital, Tongji University School of Medicine, Shanghai, PR China
[5]Department of Pathology, Fudan University Shanghai Cancer Center (FUSCC), Shanghai, PR China

*These authors contributed equally to this work.

Corresponding author:
Wei Wang, Fudan University Shanghai Cancer Center (FUSCC), Shanghai Medical College, Fudan University, 270 Dong An Road, Xuhui District, Shanghai, 200032, China.
Email: weiwang318@163.com

Keywords
Gastric schwannoma, stomach, computed tomography, clinicopathology, lymph node, exophytic growth, ulcer

Date received: 17 July 2018; accepted: 4 February 2019

Introduction

Schwannomas originate from Schwann cells of the neural sheath of peripheral nerves and most commonly occur in the head and neck or in the flexor side of the extremities.[1,2] Schwannomas rarely occur in the gastrointestinal tract and the stomach is the most common gastrointestinal site. Gastric schwannomas (GSs) represent approximately 0.2% of all gastric tumors[3,4] and 2% to 7% of all gastrointestinal mesenchymal tumors.[5,6] Conventional schwannomas are encapsulated tumors that are generally benign and have slow growth, and malignant schwannomas are extremely rare.[3,7] Schwannomas are characteristically composed of both hypercellular (Antoni type A) and hypocellular (Antoni type B) areas. In contrast, GSs are completely or predominantly composed of Antoni type A areas, which may result in different imaging features from those at other sites.[8–10] GS usually presents with non-specific symptoms, epigastric pain, or black stool.[11,12] Histological features of GS include a spindle cell pattern, usually with vague nuclear palisading and peritumoral lymphoid cuff, and without encapsulation.[13,14] A histological diagnosis of GS can be confirmed by positive immunoreactivity for S-100 protein and negative immunoreactivity for CD117 and DOG-1.[11,13,15] GS generally has a favorable prognosis, and surgical resection is considered an effective treatment.

Because of a lack of specific imaging features, GSs are difficult to be distinguished from the more common submucosal tumors, such as gastrointestinal stromal tumor (GIST), before surgery. However, the treatment and prognosis are totally different between these two tumors. Therefore, the correct diagnosis of GS before surgery is important in these patients.

In this study, we retrospectively studied 19 patients with GS. We evaluated CT and clinicopathological parameters to determine the characteristics of tumors and to diagnose GS accurately before surgery.

Materials and methods

Patients

We retrospectively reviewed the clinical features and CT findings of 19 patients who were admitted to Fudan University Shanghai Cancer Center (FUSCC) and Tongji University Shanghai East hospital-with pathologically proven GS from January 2010 to December 2015. All 19 patients underwent a CT scan and surgical removal of the tumor in our hospitals. The study was approved by the Ethics Committees of our centers of Fudan University and Tongji University. Written informed consent was waived because of the retrospective nature of the study.

CT protocol

Fourteen patients were screened using a multidetector spiral CT (Sensation 64; Siemens Medical Systems, Forchheim, Germany) in FUSCC. Images were obtained at 120 kV and 200 mA with

1-mm slice thickness. Eleven of 14 patients underwent plain (non-contrast) and dynamic contrast scans (including arterial and portal phases). Contrast images were acquired in the arterial and portal phases. The delay time of the contrast-enhanced CT images was 30 to 35 seconds for the arterial phase and 65 to 70 seconds for the portal phase after intravenous injection of 90 mL iohexol (Omnipaque 300; Amersham, Shanghai, China) at a rate of 3 mL/second. Three patients underwent a portal scan only without plain CT.

Five patients were examined with a multidetector spiral CT (Brilliance 64, Philips Medical Systems, Cleveland, OH, USA) in Shanghai East Hospital. A plain scan with dynamic contrast imaging was conducted with 3-mm slice thickness, using Ultravist (Iopromide 300; Bracco Sine, Shanghai, China) as the contrast agent.

Image interpretation

The CT images were retrospectively evaluated on a picture archiving and communication system by two experienced gastrointestinal radiologists, and disagreements were resolved through consultation.

CT findings of tumor location, size, contour, margin, and growth pattern, ulcers, perigastric lymph nodes, degree and pattern of enhancement, hemorrhage, and necrosis and calcification in tumors were analyzed. The size of the tumor was determined according to the maximum diameter of the tumor on axial/coronal/sagittal images as measured by digital calipers. The contour of the tumor was classified as either oval or lobulated. The margin was classified as well- or ill-defined in the contrast phase. The growth pattern of the tumor was classified as exophytic, endoluminal, or mixed growth.[16] The enhancement pattern was classified as either homogeneous or heterogeneous. Contrast enhancement (in Hounsfield units [HU]) was calculated from the difference in tumor CT values between the portal phase and plain scan, and was graded as mild (<10 HU), moderate (10–40 HU), and marked (>40 HU).[16,17] A perigastric lymph node was considered positive if the shortest diameter was greater than 5 mm. Calcification was defined as a region with a density of 80 to 200 HU on a plain CT scan. Necrosis was defined as a region with low attenuation on a plain CT scan and no enhancement on an enhanced CT scan. An ulcer was defined as a gastrointestinal mucosal defect on the surface of the tumor appearing as slit- or elliptical-shaped lesions.[16]

Histopathological evaluation

All of the tumors were removed and lymph node dissection was performed. The two hospitals had different surgical procedures. Surgical resection was performed at FUSCC (n = 14) and laparoscopic resection at Shanghai East Hospital (n = 5). Specimens were obtained, and all of the tissues were fixed in 10% buffered formalin and embedded in paraffin. Immunohistochemical staining of the schwannoma-specific marker S-100 protein,[18] the gastrointestinal stromal tumor markers CD117, DOG-1, and CD34,[19] and the cell proliferation marker Ki-67[20] was performed. Immunostaining results were recorded on a semiquantitative scale, including scores for the proportion of positive cells (0 = 0%, 1 = <10%, 2 = 10%–50%, and 3 = >50%) and staining intensity (0 = negative, 1 = weak, and 2 = strong).[21]

Statistical analysis

Continuous variables are summarized as mean ± standard deviation and categorical variables are described with frequencies and percentages. Statistical analyses were performed by using SPSS (version 21.0; IBM Corp., Armonk, NY, USA).

Results

Clinical data, CT characteristics, and histopathological and immunophenotypic features of the 19 patients are shown in Tables 1 and 2. Representative patients are shown in Figures 1 to 6.

Clinical features

The mean (± standard deviation) age of the patients was 53.42 ± 10.45 years (range, 25–75 years) and the female to male ratio was 13:6 (68.4%:31.6%). The clinical manifestations included asymptomatic (n = 9, 47.4%), epigastric pain (n = 5, 26.3%), epigastric discomfort (n = 2, 10.5%), black stool (n = 2, 10.5%), and chest pain (n = 1, 5.3%). None of the patients had a history of neurofibromatosis. Asymptomatic patients were detected during medical or other examinations incidentally.

CT findings

The tumors were located in the gastric body (n = 14, 73.7%), gastric antrum (n = 3, 15.8%), and gastric fundus (n = 2, 10.5%). The mean maximum diameter of the tumors was 4.53 ± 1.84 cm (range, 2.0–7.7 cm) for the entire group. All of the 19 tumors appeared as well-defined and oval, and their growth patterns included exophytic (n = 7, 36.8%), endoluminal (n = 3, 15.8%), and mixed (n = 9, 47.4%) types (Figure 1a–d).

A dynamic contrast-enhanced CT scan was performed in 16 patients. Compared with the liver, the tumors displayed iso- to mild hypoattenuation on a plain scan. All but one (18/19, 94.7%) patient showed homogeneous enhancement in the portal phase (Figure 2). One (1/19, 5.3%) case that showed heterogeneous enhancement was due to intratumoral necrosis. Of the 16 patients who had a dynamic CT scan performed, the degree of enhancement in tumors was moderate in 14 (87.5%, range: 12.5–36.0 HU, Figure 2a, b) and marked in two (12.5%, 58.3 and 62.2 HU, Figure 2c, d). The mean CT values of GSs at three phases were 34.4 ± 6.5 HU (range, 22.4–43.0 HU), 50.6 ± 11.0 HU (range, 34.6–69.4 HU), and 65.1 ± 14.3 HU (range, 44.8–100.7 HU), respectively (Figure 6). Curvilinear calcification on the margin of the tumor was observed in one (1/16, 6.3%) patient (Figure 2c). Intratumoral hemorrhage was not observed on any of the enhanced CT scans.

Ulcers were observed on the side of the gastric lumen in 11 (11/19, 57.9%) tumors (Figure 1a, d). Of these 11 patients, six (54.5%) were asymptomatic, three (27.3%) showed epigastric pain or discomfort, one (9.1%) showed chest pain; and one (9.1%) presented with black stool. The average diameter of tumors with ulcers was approximately 5.1 cm and that of tumors without ulcers was 3.7 cm.

Perigastric lymph nodes were detected in nine (9/19, 47.4%) patients on CT images (Figure 3) and coexistence with ulcers was observed in six patients.

Histopathological and immunophenotypic features

In our study, 18 of 19 patients with GS had preoperative gastroscopy (n = 18) and endosonography (n = 8) performed. Among these patients, four underwent preoperative biopsy whose pathological results (without immunohistochemistry results) included spindle cell tumor (n = 2) and chronic inflammation (n = 2). The clinical diagnoses of all 19 patients before surgery included GIST (n = 13), submucosal tumor (n = 5), and leiomyoma (n = 1) according to the results of endoscopy, clinical materials, or CT.

Gross specimens showed only one tumor with a capsule. Under microscopic examination, the tumors consisted entirely or mainly of short spindle-shaped cells with

Table 1. CT and clinical features of 19 cases with gastric schwannoma.

No.	Sex/age (y)	Size (cm)	Site	Clinical presentation	Contour	Margin	Growth pattern	Ulcer	PLN	En pattern	Degree of en
1	F/58	4.0	Body (lesser curvature)	Asymptomatic	Oval	WD	Exophytic	Yes	Yes	Homo	Marked
2	F/56	7.3	Fundus (posterior wall)	Epigastric pain	Oval	WD	Mixed	Yes	Yes	Homo	Moderate
3	M/50	5.6	Body (lesser curvature)	Chest pain	Oval	WD	Endoluminal	Yes	Yes	Homo	Moderate
4	F/43	4.0	Body (lesser curvature)	Asymptomatic	Oval	WD	Exophytic	No	No	Homo	Moderate
5	F/63	2.0	Fundus (posterior wall)	Epigastric pain	Oval	WD	Exophytic	No	No	Homo	Moderate
6	F/57	7.0	Body (greater curvature)	Epigastric discomfort	Oval	WD	Exophytic	No	No	Hetero	None
7	M/25	3.5	Antrum (lesser curvature)	Asymptomatic	Oval	WD	Endoluminal	No	Yes	Homo	Moderate
8	F/52	6.0	Body (greater curvature)	Asymptomatic	Oval	WD	Mixed	Yes	No	Homo	Moderate
9	F/54	3.2	Body (greater curvature)	Epigastric discomfort	Oval	WD	Mixed	Yes	Yes	Homo	Moderate
10	M/56	4.0	Antrum (greater curvature)	Asymptomatic	Oval	WD	Mixed	Yes	Yes	Homo	Moderate
11	F/57	3.0	Antrum (greater curvature)	Asymptomatic	Oval	WD	Exophytic	Yes	No	Homo	Moderate
12	F/60	3.5	Body (greater curvature)	Black stool	Oval	WD	Mixed	No	No	Homo	None
13	M/44	5.0	Body (lesser curvature)	Black stool	Oval	WD	Endoluminal	Yes	No	Homo	None
14	M/75	7.6	Body (lesser curvature)	Asymptomatic	Oval	WD	Mixed	Yes	Yes	Homo	Moderate
15	F/57	3.0	Body (greater curvature)	Asymptomatic	Oval	WD	Mixed	No	Yes	Homo	Moderate
16	F/64	2.0	Body (lesser curvature)	Epigastric pain	Oval	WD	Exophytic	No	No	Homo	Moderate
17	F/51	7.7	Body (greater curvature)	Asymptomatic	Oval	WD	Exophytic	Yes	No	Homo	Marked
18	M/41	4.5	Body (greater curvature)	Epigastric pain	Oval	WD	Mixed	No	Yes	Homo	Moderate
19	F/52	3.2	Body (greater curvature)	Epigastric pain	Oval	WD	Mixed	Yes	No	Homo	Moderate

No.: number of cases, y: years, F: female, M: male, WD: well-defined, PLN: perigastric lymph nodes, en: enhancement, homo: homogeneous, hetero: heterogeneous.

Table 2. Immunophenotypic features of 19 cases of gastric schwannoma.

Antibody	No. of cases examined	No. negative	No. focally positive (<10%)	No. focally positive (>10%)	No. strongly positive
S-100	19	0	0	19	19
CD117	19	19	0	0	0
DOG-1	14	14	0	0	0
CD34	14	10	4	0	0
Ki-67	12	0	12	0	0

No.: number

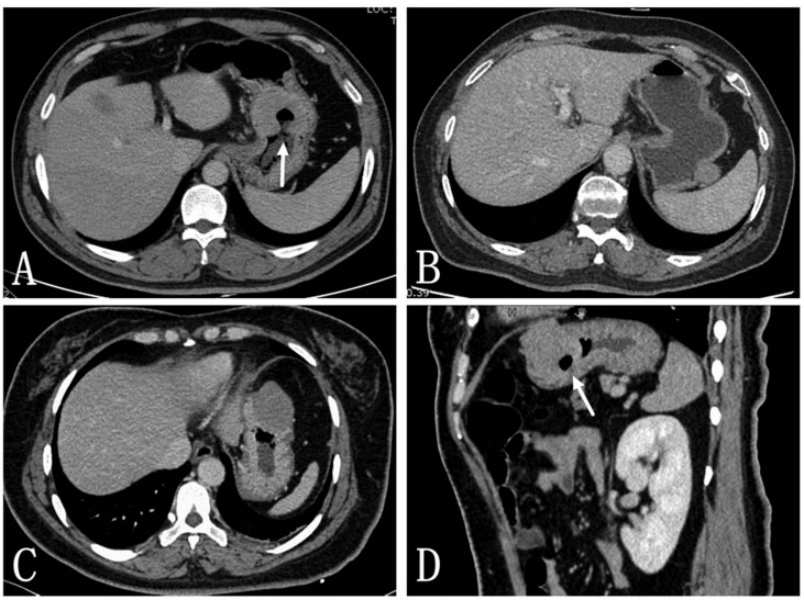

Figure 1. Portal phase-enhanced CT scans of three patients with gastric schwannomas. (a) Axial CT image shows an endoluminal tumor growth with an ulceration (arrow) in the lesser curvature of the gastric body in a 50-year-old man who presented with chest pain (Patient 3, Table 1) (b) Axial CT image shows an exophytic tumor growth in the posterior wall of the fundus in a 63-year-old woman with epigastric pain (Patient 5, Table 1). (c, d) Transverse and sagittal CT images show a mixed growth gastric schwannoma with an ulceration (arrow) in the greater curvature of the gastric body in a 52-year-old woman who presented with epigastric pain (Patient 19, Table 1). CT: computed tomography.

no nuclear atypia (Figure 4a). A peripheral lymphoid cuff (Figure 5a) and germinal center were detected in eight tumors. The number of lymph nodes was calculated after surgical resection, and it ranged from 1 to 21. The maximum shortest diameter was 15 mm. Perigastric lymph nodes that were resected during the operation showed reactive inflammatory changes without any evidence of neoplastic cells or malignancy.

Immunohistochemical analysis showed strong positive staining for S-100 protein (Figure 4b) and negative staining for CD117 in all of the patients (100%).

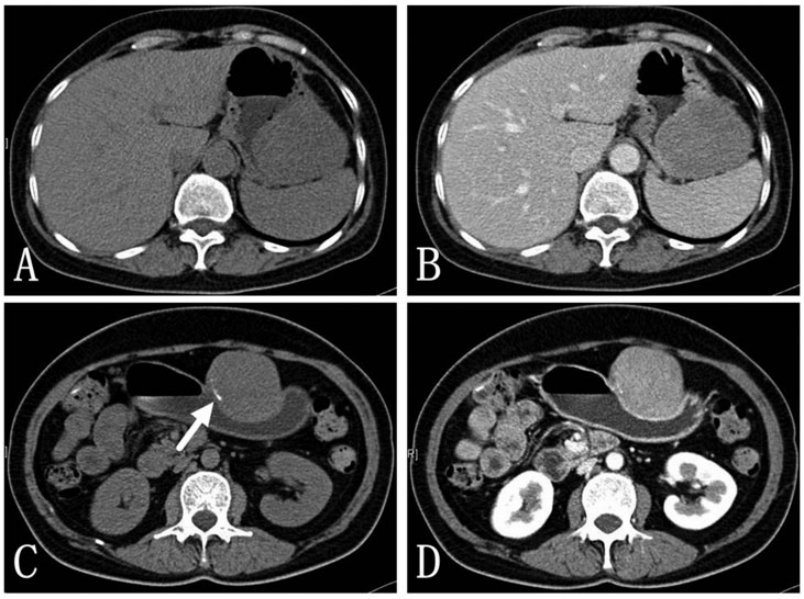

Figure 2. (a, b) A gastric schwannoma in a 56-year-old woman who presented with epigastric pain (Patient 2, Table 1). (a) A plain CT scan shows a tumor arising from the posterior wall of the gastric fundus. (b) Portal phase of the CT scan shows that the tumor is moderately, homogeneously enhanced. (c, d) A gastric schwannoma in a 51-year-old woman without any symptoms (Patient 17, Table 1). (c) A plain CT scan shows a tumor arising from the greater curvature of the gastric body, with curvilinear calcification seen at the margin of the mass (white arrow). (d) Portal phase CT scan shows that the tumor is markedly, homogeneously enhanced. CT: computed tomography.

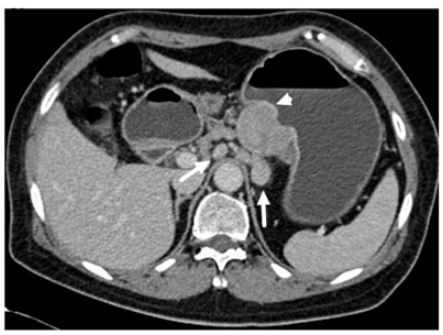

Figure 3. Axial portal phase computed tomographic image shows perigastric lymph nodes (arrow) in a 58-year-old woman with gastric schwannoma (arrow head) (Patient 1, Table 1).

DOG-1 staining was performed in 14 patients and all of these patients showed negative results. CD34 was focally expressed in minor fractions of the tumor vessels in four patients and Ki-67 was focally positive in 12 patients (Figure 5b) (Table 2).

Discussion

Previous studies have reported that GS predominantly occurs in older women.[13] Similarly, our study showed that middle-aged women had the highest incidence of GS, based on age and sex distribution of the patients. Patients with GS usually manifested no specific clinical symptoms. Almost half of the patients in this study were asymptomatic; other clinical symptoms included epigastric pain, epigastric discomfort, black stool, and chest pain.

GS is most commonly located in the gastric body. In the present study, 14 (73.7%) tumors were detected in the gastric body,

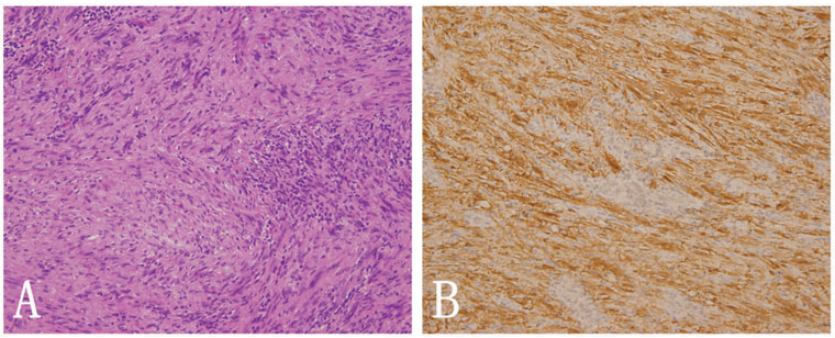

Figure 4. Histopathological and immunophenotypic features of Patient 17 (Table 1). The tumor shows (a) a biphasic pattern with cellular Antoni A and hypocellular Antoni B areas (hematoxylin and eosin stain; original magnification, ×200) and (b) S-100 positive staining in elongated tumor cells and negative staining in Antoni B areas.

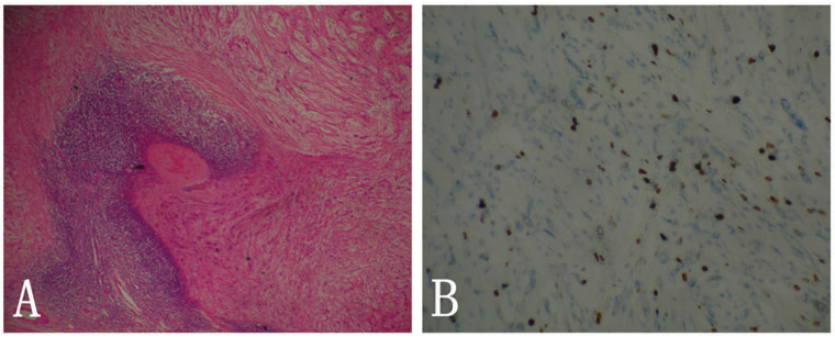

Figure 5. Histopathological and immunophenotypic features of Patient 19 (Table 1). The tumor is (a) mainly composed of spindle-shaped cells with a characteristic peripheral lymphoid cuff (hematoxylin and eosin stain; original magnification, ×100). (b) The tumor is positive (<10%) for Ki-67.

similar to rates of 56.7% and 92.9% reported in previous studies.[11,22] Our finding of a predominant exophytic and mixed growth pattern, which accounted for 84.2% of all tumors, is also consistent with previous reports.[3,17,22]

CT is a noninvasive method and is widely used in clinical examinations. GS usually shows a well-defined, oval, and iso- to mildly hypoattenuated mass compared with the liver on plain CT images,[3,23] and a homogenous enhancement pattern on enhanced CT images. GSs are slow growing and the reported mean tumor volume doubling time of 1685.4 days is much longer than that of GISTs (377.6 days).[17] According to the mean CT values of GSs in each phase in our study, GSs showed a progressive enhancement pattern (Figure 6). For the 16 patients who underwent a dynamic contrast CT scan, the tumors showed moderate to marked enhancement compared with those on plain CT, which is consistent with previous reports that GS is a richly vascularized tumor.[16,23] In contrast to conventional schwannomas, GSs lack Antoni type B areas, which contain an edematous pattern

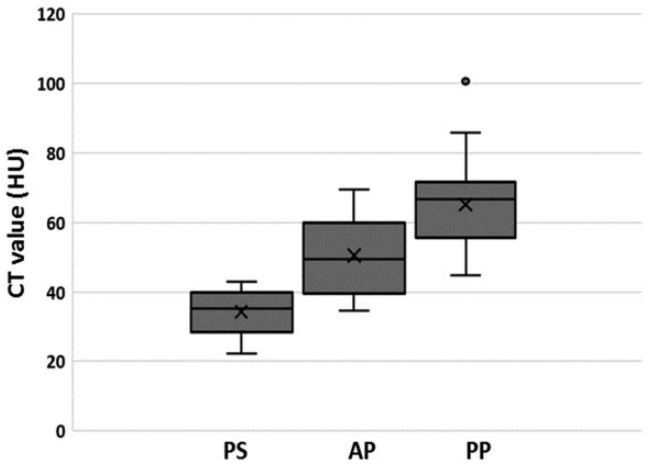

Figure 6. Graph shows computed tomographic values of 16 patients in each phase of a dynamic contrast-enhanced computed tomographic scan. PS: plain scan, AP: arterial phase, PP: portal phase.

forming cystic spaces. Because GSs are completely or predominately composed of Antoni A areas and have good blood supply, GSs rarely develop degenerative changes, such as necrosis and calcification.[11,24,25] In line with previous reports,[16] necrosis or calcification was found in only one case in the current study.

Ulcers were detected in more than 50% of the tumors in our study, which is in contrast to the lower incidence of ulcers in most previous reports.[22,26] We obtained multiplanar reconstruction using a thin layer CT scan, which visibly revealed the ulcers in some tumors. All of the ulcers were located on the luminal side of the tumor. Endoluminal or mixed growth tumors rise up and stretch the gastric mucosa, thereby reducing the blood supply of the mucosa. Consequently, a gastric mucosal ulcer may occur because of ischemia and friction of food with the mucosa. When the tumor is exposed to gastric acid, this acid can corrode the tumor and cause tissue necrosis and collapse. Tumors with an exophytic growth pattern are markedly less prone to mucosal ulceration. Indeed, only one ulcer was detected in an exophytic tumor in the present study, compared with 10 ulcers in tumors with endoluminal and mixed growth patterns. The risk of ulcers increased with the size of the tumor. Similarly, the average diameter of tumors with an ulcer (5.1 cm) was larger than that of tumors without an ulcer (3.7 cm) in our study. We also found that the incidence of GS with ulcers was 57.9% (11/19), in which the incidence of GS ($\geq$5 cm) with ulcers was 85.7% (6/7), which is higher than that in a previous report (62.5%).[27] Nonetheless, ulcers sometimes did not cause clinical symptoms. In our study, six patients with ulcers were asymptomatic and occasionally GSs were detected in physical or other examinations. Among the 11 patients with ulcers, only one patient showed black stool and this symptom disappeared after the tumor was resected.

In previous reports, the incidence of GS with peritumoral lymph nodes ranged from 67% (10/15)[16] to 81% (13/16).[17] However, some reports did not mention whether there were perigastric lymph nodes. Perigastric lymph nodes were observed in nine (47.4%) patients in our study. The number of lymph nodes was counted after

surgery and the maximum number was 21. However, a fewer number of lymph nodes were detected on CT images, partly because of the difficulty in distinguishing lymph nodes from small vessels. Histopathology showed that all of the perigastric lymph nodes manifested as inflammatory reactive hyperplasia, without any evidence of neoplastic cells or malignancy. Previous reports also showed that chronic inflammatory cells infiltrated particularly within GSs and the perigastric lymph nodes were reactive inflammatory nodes.[7,17,28] Additionally, six cases with perigastric lymph nodes showed coexistence with a tumor ulcer in this study. The association between GS and enlarged perigastric lymph nodes remains unclear.

The main challenges for the diagnosis of GS are differentiation from GIST, leiomyoma, and polypoid gastric cancer (GC). GIST is the most common submucosal tumor in the stomach and most GSs can easily be misdiagnosed as GIST before surgery. The CT features of GIST are related to the tumor size. Larger GISTs often display an exophytic growth pattern, and are prone to necrosis, hemorrhage, and cystic change.[27] In contrast, smaller GISTs often lack these features and present as small hypervascular masses with marked enhancement, making differentiation from GSs difficult.[29] The differential diagnosis of GS from GIST can be narrowed down by the co-presence of perigastric lymph nodes,[27] and can be confirmed by histopathology and positive immunoreactivity for CD117. Gastric leiomyomas usually present as homogeneous hypoattenuated masses with an endoluminal growth pattern on plain CT, and show mild to moderate enhancement on contrast CT.[30,31] Another major feature of leiomyomas is involvement of gastric cardia and the esophagogastric junction.[32] Polypoid GCs usually manifest as endoluminal masses with gastric wall dimpling, vessel invagination, perigastric infiltration, transmural wall thickening, and perigastric lymphadenopathy. Unlike GSs, GCs demonstrate marked enhancement on CT without normal mucosal coverage.[33] The precise diagnosis of GS still depends on immunohistochemical results, such as positive S-100 staining, and negative CD117 and DOG-1 staining. Therefore, immunohistochemistry is necessary for differential diagnosis with other tumors.

Our study has several limitations. First, this study used a retrospective design and thus the use of varying CT scanners and selection bias were inevitable. Second, for some patients with poor dilatation of the stomach during CT scans, misdiagnosis could have been made because of misjudgment of the growth pattern of the tumor on CT images. Finally, no comparison was made with other gastric tumors, such as GIST and leiomyomas. Well-designed prospective studies are required to address these limitations in the future.

In conclusion, GS usually appears as a benign submucosal tumor in the stomach with an exophytic or mixed growth pattern, and moderate homogeneous enhancement on CT. GS frequently co-occurs with swelling perigastric lymph nodes. Larger GSs might be more likely to be associated with ulcers. This study shows the CT features of GS, which could aid in the diagnosis of this disease.

Declaration of conflicting interest

The authors declare that there is no conflict of interest.

Funding

This research received no specific grant from any funding agency in the public, commercial, or not-for-profit sectors.

ORCID iD

Wei Wang http://orcid.org/0000-0002-2712-6186

References

1. Young ED, Ingram D, Metcalf-Doetsch W, et al. Clinicopathological variables of sporadic schwannomas of peripheral nerve in 291 patients and expression of biologically relevant markers. *J Neurosurg* 2018; 129: 805–814.
2. Das GTK, Brasfield RD, Strong EW, et al. Benign solitary Schwannomas (neurilemomas). *Cancer* 1969; 24: 355–366.
3. Hong HS, Ha HK, Won HJ, et al. Gastric schwannomas: radiological features with endoscopic and pathological correlation. *Clin Radiol* 2008; 63: 536–542.
4. Daimaru Y, Kido H, Hashimoto H, et al. Benign schwannoma of the gastrointestinal tract: a clinicopathologic and immunohistochemical study. *Hum Pathol* 1988; 19: 257–264.
5. Goh BK, Chow PK, Kesavan S, et al. Intraabdominal schwannomas: a single institution experience. *J Gastrointest Surg* 2008; 12: 756–760.
6. Agaimy A, Markl B, Kitz J, et al. Peripheral nerve sheath tumors of the gastrointestinal tract: a multicenter study of 58 patients including NF1-associated gastric schwannoma and unusual morphologic variants. *Virchows Arch* 2010; 456: 411–422.
7. Hilton DA and Hanemann CO. Schwannomas and their pathogenesis. *Brain Pathol* 2014; 24: 205–220.
8. Moriya T, Kimura W, Hirai I, et al. Pancreatic schwannoma: case report and an updated 30-year review of the literature yielding 47 cases. *World J Gastroenterol* 2012; 18: 1538–1544.
9. Rodriguez FJ, Folpe AL, Giannini C, et al. Pathology of peripheral nerve sheath tumors: diagnostic overview and update on selected diagnostic problems. *Acta Neuropathol* 2012; 123: 295–319.
10. Lee NJ, Hruban RH and Fishman EK. Abdominal schwannomas: review of imaging findings and pathology. *Abdom Radiol (NY)* 2017; 42: 1864–1870.
11. Tao K, Chang W, Zhao E, et al. Clinicopathologic features of gastric schwannoma: 8-year experience at a single institution in China. *Medicine (Baltimore)* 2015; 94: e1970.
12. Zheng L, Wu X, Kreis ME, et al. Clinicopathological and immunohistochemical characterisation of gastric schwannomas in 29 cases. *Gastroenterol Res Pract* 2014; 2014: 202960.
13. Voltaggio L, Murray R, Lasota J, et al. Gastric schwannoma: a clinicopathologic study of 51 cases and critical review of the literature. *Hum Pathol* 2012; 43: 650–659.
14. Rodriguez E, Tellschow S, Steinberg DM, et al. Cytologic findings of gastric schwannoma: a case report. *Diagn Cytopathol* 2014; 42: 177–180.
15. Takemura M, Yoshida K, Takii M, et al. Gastric malignant schwannoma presenting with upper gastrointestinal bleeding: a case report. *J Med Case Rep* 2012; 6: 37.
16. He MY, Zhang R, Peng Z, et al. Differentiation between gastrointestinal schwannomas and gastrointestinal stromal tumors by computed tomography. *Oncol Lett* 2017; 13: 3746–3752.
17. Choi JW, Choi D, Kim KM, et al. Small submucosal tumors of the stomach: differentiation of gastric schwannoma from gastrointestinal stromal tumor with CT. *Korean J Radiol* 2012; 13: 425–433.
18. Sarlomo-Rikala M and Miettinen M. Gastric schwannoma–a clinicopathological analysis of six cases. *Histopathology* 1995; 27: 355–360.
19. Swalchick W, Shamekh R and Bui MM. Is DOG1 immunoreactivity specific to gastrointestinal stromal tumor. *Cancer Control* 2015; 22: 498–504.
20. Ko GH, Go SI, Lee WS, et al. Prognostic impact of Ki-67 in patients with gastric cancer-the importance of depth of invasion and histologic differentiation. *Medicine (Baltimore)* 2017; 96: e7181.
21. Isabel ZY and Fitzpatrick JE. Expression of c-kit (CD117) in Spitz nevus and malignant melanoma. *J Cutan Pathol* 2006; 33: 33–37.
22. Fujiwara S, Nakajima K, Nishida T, et al. Gastric schwannomas revisited: has precise preoperative diagnosis become feasible. *Gastric Cancer* 2013; 16: 318–323.
23. Ji JS, Lu CY, Mao WB, et al. Gastric schwannoma: CT findings and clinicopathologic correlation. *Abdom Imaging* 2015; 40: 1164–1169.

24. Rha SE, Byun JY, Jung SE, et al. Neurogenic tumors in the abdomen: tumor types and imaging characteristics. *Radiographics* 2003; 23: 29–43.
25. Chetty R. Reticular and microcystic schwannoma: a distinctive tumor of the gastrointestinal tract. *Ann Diagn Pathol* 2011; 15: 198–201.
26. Kwon MS, Lee SS and Ahn GH. Schwannomas of the gastrointestinal tract: clinicopathological features of 12 cases including a case of esophageal tumor compared with those of gastrointestinal stromal tumors and leiomyomas of the gastrointestinal tract. *Pathol Res Pract* 2002; 198: 605–613.
27. Choi YR, Kim SH, Kim SA, et al. Differentiation of large (>/=5 cm) gastrointestinal stromal tumors from benign subepithelial tumors in the stomach: radiologists' performance using CT. *Eur J Radiol* 2014; 83: 250–260.
28. Shimizu S, Saito H, Kono Y, et al. Gastric schwannoma with enlargement of the regional lymph nodes resected using laparoscopic distal gastrectomy: report of a patient. *Yonago Acta Med* 2017; 60: 59–63.
29. Johnson PT, Horton KM and Fishman EK. Hypervascular gastric masses: CT findings and clinical correlates. *AJR Am J Roentgenol* 2010; 195: W415–W420.
30. Lee MJ, Lim JS, Kwon JE, et al. Gastric true leiomyoma: computed tomographic findings and pathological correlation. *J Comput Assist Tomogr* 2007; 31: 204–208.
31. Kang HC, Menias CO, Gaballah AH, et al. Beyond the GIST: mesenchymal tumors of the stomach. *Radiographics* 2013; 33: 1673–1690.
32. Yang HK, Kim YH, Lee YJ, et al. Leiomyomas in the gastric cardia: CT findings and differentiation from gastrointestinal stromal tumors. *Eur J Radiol* 2015; 84: 1694–1700.
33. Lee ES, Kim SH, Lee JY, et al. Radiologist performance in differentiating polypoid early from advanced gastric cancer using specific CT criteria: emphasis on dimpling sign. *AJR Am J Roentgenol* 2009; 193: 1546–1555.